Bandwidth Enhancement of the Cavity Resonance Antenna (CRA) Using Multiple Dielectric Superstrate Layers

Muhannad A. Al-Tarifi, Dimitris E. Anagnostou, Anthony K. Amert, and Keith W. Whites

South Dakota School of Mines and Technology, Rapid City, South Dakota, 57701, US

***Abstract* — The ray-tracing method is applied to study the radiation of a cavity resonance antenna (CRA) with both single and multiple dielectric superstrate layers. The behavior of the broadside directivity is investigated by analyzing the reflection phase of the antenna superstrates. To enhance the bandwidth of the CRA and maintain its large broadside directivity, a multilayered superstrate of an increasing reflection phase with frequency is presented. When compared to the single-layered CRA, a bandwidth enhancement of more than 100% is attained using a multilayered CRA of three superstrate slabs. Theoretical results are validated by simulations using commercial numerical electromagnetics software.**

***Index Terms* — Broadband antennas, cavity resonators, directive antennas, electromagnetic propagation, electromagnetic reflection, leaky wave antennas.**

I. Introduction

A dielectric slab can be used as a superstrate layer above a broadside feed placed next to a flat ground plane to increase its directivity [1]. Due to simplicity and low cost, this type of high gain antenna has attracted significant attention in the last few decades, and many theoretical approaches have been presented to analyze the radiation characteristics of such structures [1] - [4]. The ray-tracing method has been widely used to simplify the structure to a cavity resonance model [3]. In this method, rays are fed into the structure and undergo multiple reflections inside the cavity formed by the ground and the superstrate planes, which leads to this device being named a cavity resonance antenna (CRA). The total radiation is calculated by summing of the wave portions transmitted through the superstrate after each reflection, where the superstrate acts as a partially reflecting surface (PRS). The most of the radiation is directed toward the angle where the transmitted portions of the beams are in-phase. Traditionally, the broadside directivity by a single-layered CRA has a narrow bandwidth; therefore, many techniques to enhance the bandwidth have been conceived by many research groups in the recent years [5]-[6].

This paper analyzes a CRA with a dielectric superstrate layer using the ray-tracing method and provides useful observations on the antenna radiation patterns, broadside directivity, and phase variations with frequency. Next, the analysis is extended to the CRA with multiple superstrate layers that are treated as a single PRS. The added layers introduce more variables to the CRA design. For a suitable assortment of these variables, a superstrate reflection phase that increases with frequency can be established. It will be shown that this phase behavior enhances the bandwidth of the CRA broadside directivity while it maintains its maximum value within 3 dB of the maximum broadside directivity obtained by the single-layered CRA.

II. CRA with a Single Superstrate Layer

Fig. 1a shows the geometry of a single-layered CRA, where a horizontal infinitesimal dipole feeds the cavity formed by a high permittivity planar dielectric layer of thickness *t*, placed a distance *h* above a perfect electric conductor (PEC) ground plane. The structure is assumed lossless and infinite in the *x*-*y* plane.

A ray-tracing diagram of the geometry is shown in Fig. 1b. The radiated wave from the feed antenna impinges on the superstrate, partially reflects, and partially transmits. By taking into account all phase shifts caused by the multiple reflections of the rays and by the travel distance of the rays between the superstrate and the PEC, an expression for the transmission pattern radiated out of the structure assuming an isotropic feed is derived as [3]

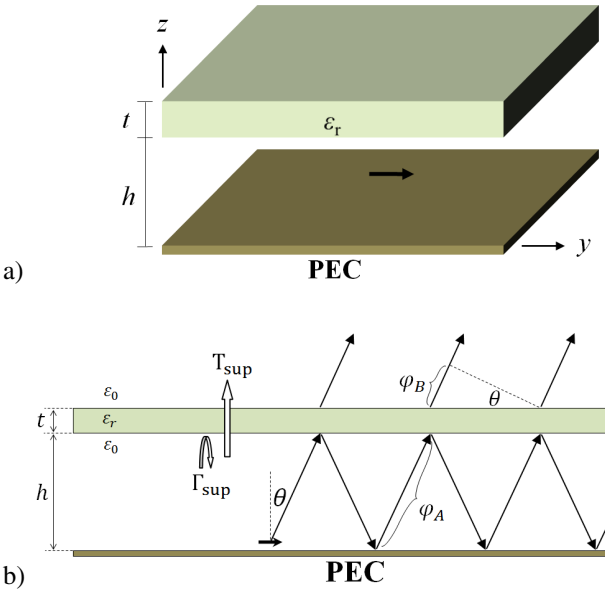

Fig. 1. (a) A single superstrate layer CRA, and (b) ray-tracing method for radiation analysis. A horizontal infinitesimal dipole feed is assumed.

978-1-61284-757-3/11/$26.00 C2011 IEEE

$$T_{cavity} = \frac{T_{sup}}{1+\Gamma_{sup}e^{-j2\varphi_A}e^{j\varphi_B}} \quad (1)$$

$$\varphi_A = kh/\cos\theta$$
$$\varphi_B = 2kh\tan\theta\sin\theta$$

where Γ_{sup} and T_{sup} represent the reflection and transmission coefficients of a plane wave incident on the superstrate layer, respectively. As verified later, the assumption of a plane wave impinging upon the superstrate yields a quite accurate far-field pattern of the CRA. The total reflection and transmission coefficients of a plane wave through the superstrate layer in Fig. 1b are expressed as [7]

$$\Gamma_{sup} = \frac{\Gamma_{0,s}(1-e^{j2\phi_s})}{1-\Gamma_{0,s}^2 e^{j2\phi_s}} \quad (2)$$

$$T_{sup} = \frac{(1-\Gamma_{0,s}^2)e^{j2\phi_s}}{1-\Gamma_{0,s}^2 e^{j2\phi_s}} \quad (3)$$

$$\phi_s = k_s t\cos\theta_s$$

where θ_s is the angle of refraction in the superstrate layer, and $\Gamma_{0,s}$ is the interface semi-infinite reflection coefficient of a plane wave propagating from free space to the superstrate.

To find the total radiation of the CRA that is fed by an infinitesimal dipole, the cavity transmission factor (T_{cavity}) is multiplied by the feed's element factor ($\mathbf{E}_{feed}$) as

$$\mathbf{E}_{total} = T_{cavity}\cdot\mathbf{E}_{feed} \quad (4)$$

At a specific frequency, the broadside radiation can be maximized by minimizing the magnitude of the denominator of (1) for θ=0. This can be obtained by maximizing $|\Gamma_{sup}|$ and forcing the phase of the second term of the denominator ($\Gamma_{sup}e^{-j2\varphi_A}e^{j\varphi_B}$) to sum to π. Fig. 2 shows the broadside reflection and transmission coefficients versus the thickness of a superstrate layer with relative permittivity of 10.8. A quarter-wavelength thickness of the superstrate layer (t) yields a maximum reflection coefficient magnitude. With this thickness, the reflection phase of the superstrate layer (φ_Γ) is π. As a result, a half-wavelength spacing from the PEC (h) minimizes the denominator in (1) and, hence, maximizes the broadside radiation. These specifications ($t=\lambda_{sup}/4$ and $h=\lambda_0/2$) are the same resonance conditions found in literature by various analytical approaches [1]-[2]. The higher resonance conditions are ignored in the current discussion due to the CRA higher profiles and the possibility of grating lobes appearance [2].

The main drawback of CRAs is the fast degradation of their radiation patterns with frequency. As the operating frequency (f) deviates from the design frequency (f_0), the variations of φ_Γ, φ_A, and φ_B result in a change in the phase resonance condition for maximum broadside radiation ($\varphi_\Gamma - 2\varphi_A + \varphi_B = \pi$). As an example to demonstrate this behavior, a CRA designed at $f=f_0$ with a $0.25\lambda_{sup}$-thick (t) superstrate of ε_r=10.8 placed at a $\lambda_0/2$ spacing (h) from the PEC plane is examined. The horizontal infinitesimal dipole feed is placed $\lambda_0/20$ above the PEC. Fig. 3 shows the broadside phase versus frequency curves. At $f=f_0$, the total phase sum is π, which coincides with the aforementioned phase resonance condition at the design frequency. However, the total phase is increasingly deviating from the phase resonance condition when the frequency is departing from f_0. Such phase behavior has an extreme deteriorating effect on the radiation pattern of the CRA, even for small changes in frequency. Fig. 4 presents the E- and H-plane directivity radiation patterns at some specific frequencies, which clearly illustrates the narrow bandwidth of the CRA broadside radiation. It is shown that simulation results by IE3D at resonance are in good agreement with the analytical results.

III. Multilayered Superstrate CRA

The total radiation analysis of a multilayered CRA is similar to the single-layered CRA. However, in this work, the reflection and transmission coefficients of the *multilayer* superstrate are used, instead of the formulas in (2) and (3) that were found for a *single* superstrate layer. These coefficients can be determined by following a recursive algorithm established in [8]. Presuming the multilayer structure in Fig. 5, the recursive formulas are

$$\Gamma_{j-1,N+1} = \Gamma_{j-1,j} + \frac{T_{j,j-1}T_{j-1,j}\Gamma_{j,N+1}e^{j2\phi_j}}{1-\Gamma_{j,N+1}\Gamma_{j,j-1}e^{j2\phi_j}} \quad (5)$$

$$T_{N+1,j-1} = \frac{T_{j,j-1}T_{N+1,j}e^{j\phi_j}}{1-\Gamma_{j,N+1}\Gamma_{j,j-1}e^{j2\phi_j}} \quad (6)$$

$$\phi_j = k_j t_j\cos\theta_j$$

Here, θ_j is the angle of refraction in layer j, where j is an integer applied to each layer using the values from N to 1. Also, $\Gamma_{i,k}$ and $T_{k,i}$ represent, respectively, the reflection and transmission coefficients of a wave propagating from medium i to medium k. The total reflection and transmission coefficients between medium 0 and medium N+1 are the last recursive evaluation (i.e. j=1) of (5) and (6), respectively. These are Γ_{sup} and T_{sup} that are applied in (1) when the multilayer structure in Fig. 5 is applied as a superstrate in a CRA. The total radiation is calculated using (4) afterwards.

When dielectric slabs are added to the superstrate layers, the dielectric constant and thickness of each slab introduce two additional design variables to the CRA design. By assuming fixed dielectric constants of the slabs, various selections of their thicknesses lead to a different behavior of the superstrate reflection and transmission coefficients. At certain cases, the reflection phase increases with frequency, which results in a bandwidth enhancement of the CRA as discussed next.

978-1-61284-757-3/11/$26.00 C2011 IEEE

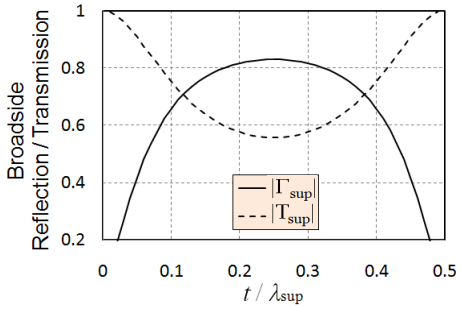

Fig. 2. Magnitudes of the broadside reflection and transmission coefficients versus the electrical thickness of a planar dielectric layer of ε_r =10.8 embedded in free space. An incident plane wave is assumed.

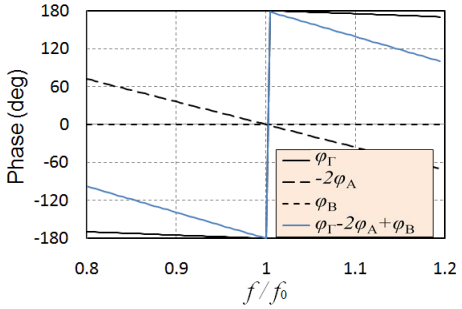

Fig. 3. Broadside variations with frequency of the phase shifts illustrated in Fig. 1(b) and evaluated in (1). ε_r =10.8, $h = \lambda_0\,(f=f_0)$ /2, and $t = \lambda_{sup}\,(f=f_0)$ /4.

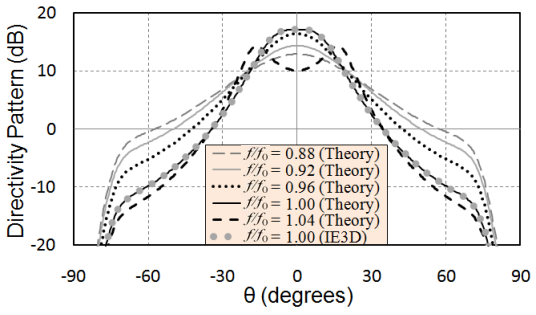

a)

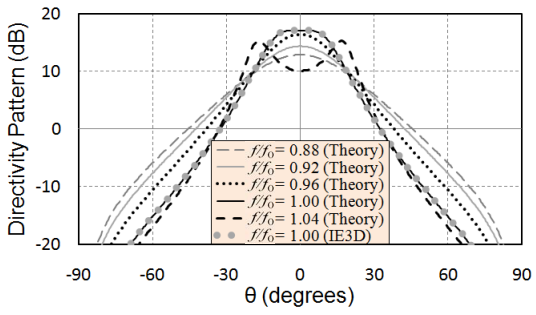

b)

Fig. 4. (a) E- and (b) H-plane directivity patterns at specific frequency points for the CRA in Fig. 1(a) using ε_r =10.8, $h = \lambda_0\,(f=f_0)$ /2, $t = \lambda_{sup}\,(f=f_0)$ /4, and $\lambda_0\,(f=f_0)$ /20 feed-PEC spacing.

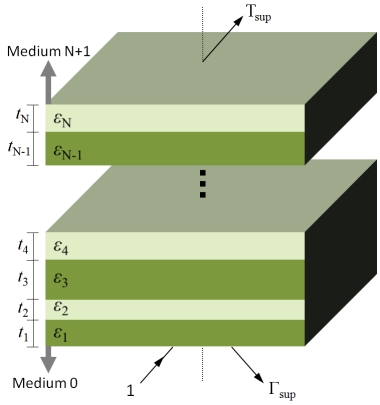

Fig. 5. *N*-layers of infinite, planar, and lossless stacked dielectrics.

IV. Bandwidth Enhancement

Fig. 6 depicts a multilayered CRA with three superstrate layers. This structure is constructed by adding a dielectric layer (ε_r) above the superstrate layer in the single-layered CRA (shown in Fig. 1) but with a free space separation between them. Here, ε_r =10.8 is assumed and the first superstrate layer thickness and spacing from the PEC are kept unchanged (i.e. $t_1 = \lambda_{sup}\,(f=f_0)$ /4 and $h = \lambda_0\,(f=f_0)$ /2). The thickness of each remaining layer (t_2 and t_3) is varied and the bandwidth of the CRA broadside directivity is observed.

The effect of the variables t_2 and t_3 is examined by a heuristic procedure. Several sets of these variables produced substantial bandwidth enhancements of the CRA broadside directivity. As an example, more than 100% enhancement is achieved when $t_2 = 2\,\lambda_0\,(f=f_0)$ /5 and $t_3 = \lambda_{sup}\,(f=f_0)$ /2 are used.

The bandwidth enhancement seen using the indicated design parameters is evaluated by observing the behavior of φ_Γ with frequency. Fig. 7 compares the broadside φ_Γ versus frequency of the single-layered and multilayered superstrate. As frequency increases, the increasing φ_Γ of the multilayered superstrate compensates for the decreasing $-2\,\varphi_A$ (shown in Fig. 3), which reduces the total phase deviation from the phase resonance condition for maximum broadside radiation of the CRA. Fig. 8 shows the directivity patterns for the multilayered CRA at selected frequency points. Compared to the single-layered CRA patterns (shown in Fig. 4), the multilayered CRA patterns show less sensitivity to frequency and, hence, an enhanced bandwidth. The directivity curves in Fig. 9 illustrate the substantial 3-dB bandwidth enhancement for the presented multilayered CRA with respect to the single-layered CRA. For the single-layered CRA, the maximum directivity is 17.7 dB and the 3-dB bandwidth is 9.1%, while for the multilayered CRA, they were 17.3 dB and 18.3%, respectively. The tradeoffs for the bandwidth enhancement are a slight drop of maximum directivity and a higher profile. Simulation results from IE3D™ match closely with the theoretical results, which verifies the accuracy of performing the ray-tracing analysis to the CRA structure, with the superstrate modeled as a PRS.

978-1-61284-757-3/11/$26.00 C2011 IEEE

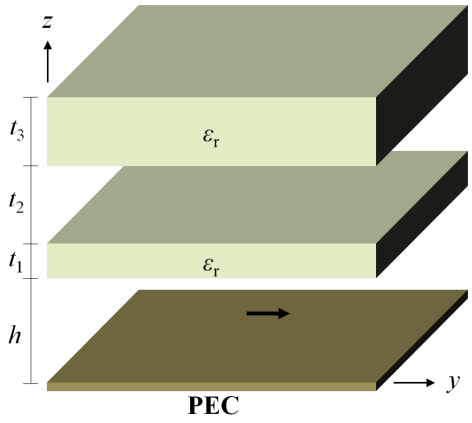

Fig. 6. A multiple superstrate layers CRA.

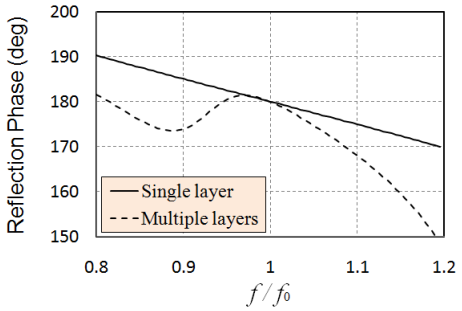

Fig. 7. Broadside reflection phase versus frequency curves of the single and multilayered superstrates in Fig. 1 and 6, respectively.

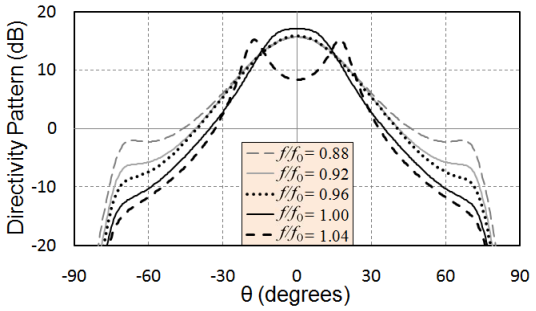

a)

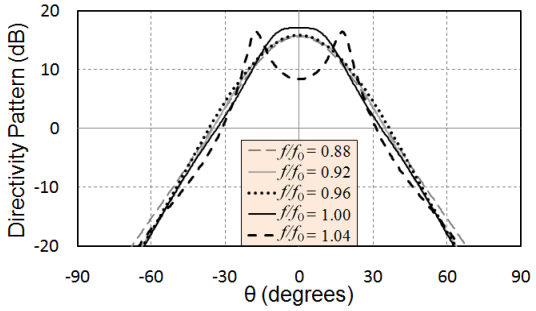

b)

Fig. 8. Theoretical (a) E- and (b) H-plane directivity patterns at specific frequency points for the CRA in Fig. 6 using ε_r =10.8, h= λ_0 (f=f_0) /2, t_1= λ_{sup} (f=f_0) /4, t_2=0.8h, t_3=2t_1, and λ_0 (f=f_0) /20 feed-PEC spacing.

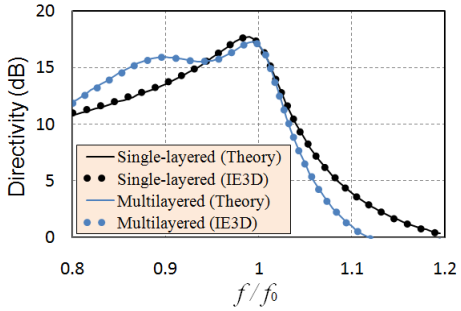

Fig. 9. Broadside directivity versus frequency curves of the single-layered and multilayered CRAs in Fig. 1 and 6, respectively.

V. Conclusions

A generalized method for analyzing a multilayered CRA with multiple dielectric superstrate layers was developed and validated in simulation. The method was applied to a multilayered CRA with three superstrate layers to enhance the bandwidth of the broadside directivity. When compared to the single-layered CRA, more than 100% bandwidth enhancement was achieved but, in compromise, the maximum directivity was dropped by 0.4 dB and the volume was approximately doubled. A close match between the theoretical results and the full wave simulations was observed.

Acknowledgement

This work was supported in part by the National Science Foundation Grant No. 0824034, by the National Science Foundation/EPSCoR Grant No. 0903804, by the DoD ARO Grant W911NF-09-1-0277, and by the NASA under Cooperative Agreement NNX07AL04A.

References

[1] D. R. Jackson, and N. G. Alexopoulos, "Gain enhancement methods for printed circuit antennas," *IEEE Trans. Antennas Propag.,* vol. AP-33, no. 9, pp. 976-987, September 1985.

[2] D. R. Jackson, and A. A. Oliner, "A leaky-wave analysis of the high gain antenna printed antenna configuration," *IEEE Trans. Antennas Propag.,* vol. 36, no. 7, pp. 905-910, July 1988.

[3] G. V. Trentini, "Partially reflecting sheet arrays," *IRE Trans. Antennas Propag.,* vol. AP-4, pp. 666-671, October 1956.

[4] G. Lovat, P. Burghignoli, F. Capolino, and D. R. Jackson, "Highly-directive planar leaky-wave antennas: a comparison metamaterial-based and conventional designs," *Proc. Eur. Microw. Association*, vol. 2, no. 1, pp. 12-21, March 2006.

[5] Y. Li, and K. P. Esselle, "Consideration of bandwidth of the small EBG-resonator antenna using the in-phase highly-reflecting surfaces," 2009 *IEEE AP-S Int. Symp.,* June 2009.

[6] A. P. Feresidis, and J. C. Vardaxoglou, "A broadband high-gain resonant cavity antenna with single feed," 2006 EuCAP, Nice, France, November 2006.

[7] C. A. Balanis, *Advanced Engineering Electromagnetics*, Ch.5. New York: J. Wiley & Sons, 1989.

[8] W. C. Chew, *Waves and Fields in Inhomogeneous Media*, Ch.2. New York: Van Nostrand, 1990.